Macromolecular Bioscience
www.mbs-journal.de

Multivalent Protein-Loaded pH-Stable Polymersomes: First Step toward Protein Targeted Therapeutics

Silvia Moreno, Susanne Boye, Hane George Al Ajeilat, Susanne Michen, Stefanie Tietze, Brigitte Voit, Albena Lederer, Achim Temme, and Dietmar Appelhans**

Synthetic platforms for mimicking artificial organelles or for designing multivalent protein therapeutics for targeting cell surface, extracellular matrix, and tissues are in the focus of this study. Furthermore, the availability of a multi-functionalized and stimuli-responsive carrier system is required that can be used for sequential in situ and/or post loading of different proteins combined with post-functionalization steps. Until now, polymersomes exhibit excellent key characteristics to fulfill those requirements, which allow specific transport of proteins and the integration of proteins in different locations of polymeric vesicles. Herein, different approaches to fabricate multivalent protein-loaded, pH-responsive, and pH-stable polymersomes are shown, where a combination of therapeutic action and targeting can be achieved, by first choosing two model proteins such as human serum albumin and avidin. Validation of the molecular parameters of the multivalent biohybrids is performed by dynamic light scattering, cryo-TEM, fluorescence spectroscopy, and asymmetrical flow-field flow fractionation combined with light scattering techniques. To demonstrate targeting functions of protein-loaded polymersomes, avidin post-functionalized polymersomes are used for the molecular recognition of biotinylated cell surface receptors. These versatile protein-loaded polymersomes present new opportunities for designing sophisticated biomolecular nanoobjects in the field of (extracellular matrix) protein therapeutics.

1. Introduction

Self-assembled systems of amphiphilic macromolecules, mostly based on amphiphilic block copolymers, are nowadays applied as drug and protein delivery vehicles, nanomotors, and/or nanoreactors, since they are biocompatible and can transport hydrophilic and hydrophobic cargoes.[1–6]

Several technologies have been used to regulate the size, shape (preferred vesicles and other), surface activity, loading efficiency of cargo, and stimuli-responsiveness membrane of these engineered polymeric vehicles.[2–4,7–20] Additionally, more sophisticated polymeric vesicles have been equipped, for example, with antibodies, peptides, proteins, or aptamers to obtain desired additional properties such as a prolonged blood circulation time or selective targeting to cells or tissues.[10,17,19,21,22] Attaching targeting ligands on the surface of smart polymeric nanocontainers which are capable to deliver therapeutic bio(macro)molecules to the tissues of interest is the key request for a controlled transport of the drug.[1,23]

S. Moreno, S. Boye, B. Voit, A. Lederer, D. Appelhans
Leibniz-Institut für Polymerforschung Dresden e.V.
Hohe Straße 6, Dresden 01069, Germany
E-mail: moreno@ipfdd.de; applhans@ipfdd.de
H. G. A. Ajeilat
German Jordanian University
Amman Madaba Street, Amman 11180, Jordan
S. Michen, S. Tietze, A. Temme
Department of Neurosurgery
Section Experimental Neurosurgery/Tumor Immunology
University Hospital Carl Gustav Carus
TU Dresden
Dresden 01307, Germany
B. Voit
Faculty of Chemistry
Technische Universität Dresden
Dresden 01062, Germany
A. Lederer
Department of Chemistry and Polymer Science
Stellenbosch University
Private Bag X1, Matieland 7602, South Africa
A. Temme
German Cancer Consortium (DKTK), partner site Dresden, Germany;
German Cancer Research Center (DKFZ), Heidelberg, Germany
National Center for Tumor Diseases (NCT)
Fetscherstraße 74, Dresden 01307, Germany

DOI: 10.1002/mabi.202100102

These ligands are usually chemically attached to the vesicles through the interaction of reactive groups on the polymersomes' surface and specific groups, which are present in the ligands. For this purpose, the direct modification of various types of block copolymers is often applied to introduce functional groups.[21,24–27] However, the use of such pre-functionalized block copolymers is not advisable when the functional groups should only be present on the outer vesicle surface or when the self-assembly of the vesicle structure is disturbed by the chemical modification of a block copolymer component. Therefore, a robust method is needed to enable bio-orthogonal and highly specific functionalization of the vesicle surfaces after the self-assembly process. Moreover, the proposed functionalization strategy should allow for reliable surface characterization and precise reaction control, which is challenging for preformed self-assembled polymersome systems.[19,22,28–30]

For a convenient and reliable coupling of different functional moieties, click chemistry is widely used due to its unique reaction properties: the procedure is very efficient at mild conditions and can be carried out in aqueous environment. Click chemistry became rapidly a popular tool to functionalize the surface of biomacromolecules, including viruses, DNA, peptides, antibodies, liposomes, micelles, and nanoparticles with a wide variety of conjugates.[31–39] One of the well-established bio-orthogonal coupling approaches is the alkyne-azide cycloaddition (SPAAC) where the use of Cu(I) as a catalyst is avoided (a great advantage regarding the known undesired effects associated with copper in cell-based studies).[40,41]

In terms of stability and chemical diversity, polymeric vesicles are superior to currently marketed liposomes, however it is still necessary to improve their modification for targeting approaches, stimuli-responsiveness, and multifunctionality.[8,9] Previous own studies were focused on pH- and/or temperature-responsive, but also on light-responsive enzyme-loaded nanoreactors based on photo-crosslinked polymersomes (Psomes), hollow capsules, and their multicompartments.[42–46] For most of these reactive enzymes they were mainly enclosed into the inner cavity of the polymeric vesicles during their formation process (in situ loading),[42–44,46] that is similar to formation processes of other enzymatic nanoreactors using (non-)crosslinked Psomes.[14,28,47,48] Further own works also demonstrated i) the ability of loading and release of therapeutic hormone such as insulin,[49] ii) the loading of enzymes in Psomes through a post loading process of swollen Psomes,[50] and iii) the ability to equip the Psomes´ surface with reactive groups (azido or adamantane groups) that allow a more controlled post-(=surface)-functionalization.[51,52] A subsequent post-functionalization of the Psomes surface was achieved using covalent azide-alkyne click reaction, functionalized pH-responsive Psomes with folate targeting antennae were also reported,[15] promoting drug release in the acidified endosomal compartment.

Based on the achieved multifunctionality, co-encapsulated drugs in polymeric vesicles have shown the improvement of therapeutic action.[53–55] Similarly, the combination of two different proteins/enzymes using different locations in polymeric compartments could also offer a synergic therapeutic effect. Therefore, the aim of our study was to contribute to broaden the methodology to achieve multifunctionality in polymersome carriers based on different loading strategies such as covalent surface functionalization, non-covalent surface and/or membrane loading, and in situ loading (**Figure 1**).[56–58] Using proteins with different polarity and surface charge, this study offers valuable information on location of entrapment/encapsulation, loading efficiency, and finally targeting properties dependent on the physical and chemical properties of the protein or of protein combinations. Adequate characterization of the loading characteristics of our polymeric compartments in the nanometer dimensions provides the needed information for placing enzymes, proteins, and antibodies at different locations in the carrier which will enhance their availability and action in potential (extracellular matrix) protein therapeutics. Changing the positioning in the carrier will provide, as needed, protection of the loaded cargo, targeting of the desired pathological site, selected activation, or can offer a double therapeutic action.[2,59]

For this study the biomacromolecules, anionic human serum albumin (HSA) and cationic avidin, were used as model proteins to clarify the high versatility of azido-modified Psomes. Avidin is known as an excellent binding moiety for recognition systems and for the functionalization of other materials through the non-covalent conjugation of avidin and their derivatives with biotinylated components,[60–62] while HSA as blood plasma protein outlines a high tendency to stick on pathogenic particles in blood.[63] Post-functionalization of Psomes surfaces with HSA and avidin was used to validate the efficiency and selectivity of SPAAC versus nonspecific interactions between PEG chains and β-cyclodextrin. Versatile asymmetrical flow-field flow fractionation (AF4) combined with light scattering devices (static light scattering and dynamic light scattering (DLS); AF4-LS) was used to thoroughly characterize the differently loaded Psomes and the precursors, azido-functionalized Psomes for SPAAC conversions as previously established for complex structures.[64] Moreover, main locations of proteins were preferentially determined by the results of the multidetector AF4 and fluorescence spectroscopy.[65] Finally, the availability of avidin post-functionalized Psomes biohybrids as recognition unit (Figure 4) was verified using a HEK293T$_{huBirA\text{-}DAP12\text{-}KiBAP}$ cell line expressing a biotinylated surface receptor (Figure 5).

2. Experimental Section

2.1. Materials

If not stated otherwise, all chemicals were used as received. All chemicals, anhydrous tetrahydrofuran (THF, Sigma Aldrich), anhydrous 2-butanone (Fluka), and triethylamine (Fluka) were stored over a molecular sieve. Avidin (egg white, ThermoFisher Scientific), Biotin-DOOA*HCl (IrishBiotec), poly(ethylene glycol) methyl ether (MeO-PEG-OH; M_n = 2000 g mol^{-1}; M_w/M_n = 1.05), azide-terminated poly(ethylene glycol) (N_3PEG-OH; M_n = 2700 g.mol^{-1}), albumin from human serum (HSA), 2-(*N,N*′diethylamino)ethyl methacrylate (DEAEM), 2,2-′bipyridine, 2-bromoisobutyryl bromide, 2-aminoethanol, 4-aminobutanol, methacryloylic chloride, copper-I-bromide, aluminum oxide (neutral, activated), phosphate buffered saline (tablet),

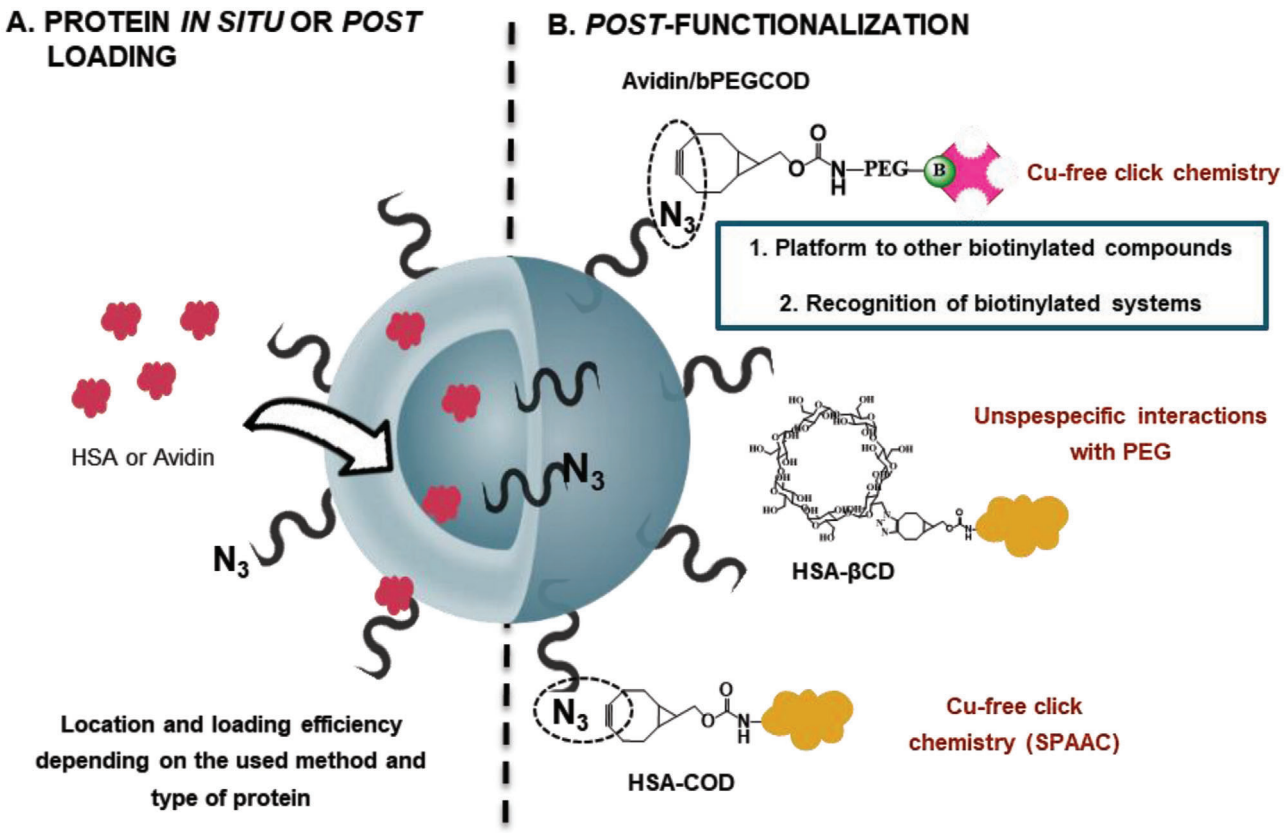

Figure 1. Scheme representation ofdifferent loading and functionalization approaches for the fabrication of protein-loaded and -decorated Psomes as protein therapeutics and diverse cell biomimetics. A) In situ and post loading of azido-(N_3)-modified Psomes using native proteins (HSA or avidin); B) post-functionalization of azido-modified Psomes using modified proteins (βCOD or avidin/bPEGCOD by SPAAC; HSA-β-CD by non-covalently driven interactions).

(1*R*,8*S*,9*s*)-Bicyclo[6.1.0]non-4-yn-9-ylmethyl *N*-succinimidyl carbonate (COD), fluorescein-5(6)-isothiocyanat (FITC), sodium hydroxide, and magnesium sulfate were purchased from Sigma Aldrich. 3,4-Dimethylmaleic acid anhydride, THF, toluene, chloroform-*d*, and ethyl acetate were purchased from Acros Organics. From Merck (Germany) *n*-hexane, hydrochloric acid (37%) and silica gel were purchased. 6-Monodeoxy-6-monoamino-β-cyclodextrin was purchased from Cyclodextrin Shop (Division of AraChem, Netherlands). AlamarBlue (cell viability reagent) and avidin (egg white) were obtained from Thermo Fisher Scientific.

2.2. Methods

All analytical methods and devices used for all characterization are presented in the Supporting Information.

2.3. Fabrication of Materials

Details about the syntheses and characterization of used block copolymers, preparation of empty polymersomes (Empty-Psomes) and modified proteins can be found in the Supporting Information (Figure S1, Table S1, Supporting Information).[43,65]

2.3.1. Fabrication of Protein-Loaded Psomes Using Post and In Situ Loading

Protein (avidin or HSA) In Situ Loaded Psomes, Using Psomes C Composition (20% N_3 = BCP2): For the in situ loading of protein *the* method of Gräfe et al. was adopted and modified for HSA or avidin.[43] 10.5 mg of BCP1 was dissolved in 10.5 mL of 10 mM hydrochloric acid (pH 2) (C_{BCP1} = 1 mg mL^{-1}) and 3 mg BCP2 in 1.5 mL in 10 mM hydrochloric acid (pH 2) (2 µg mL^{-1} pH 2). Both solutions were combined after complete dissolving and after pass through a 0.2 µm nylon filter. Then, 9.8 mL of BCP1, 1.2 mL of BCP2, and 1 mL of protein solution (1.2 mg mL^{-1}). Then, the pH was adjusted to pH 9 by adding NaOH slowly. The final block copolymer concentration must be of 1 mg mL^{-1} and the protein concentration of 0.1 mg mL^{-1}. Then, the solution was stirred for 3 days. To receive crosslinked Psomes, the solution was placed in the UV-chamber which was irradiated for 180 s. The resulting solution was cleaned from non-enclosed protein using HFF (1 mM PBS buffer at pH 8, MWCO of 500 kDa, V_{waste} = 150 mL, 150 mbar). This protocol was used for HSA, Avidin, HSA-FITC, and Avidin/bFITC.

Protein (avidin or HSA) Post Loaded Psomes, Using Psomes C Composition: 6 mL of N_3-modified polymersome (1 mg BCP per mL) was added to 5.5 mL of 2 mM PBS. The pH was adjusted to pH 6. Then, 0.5 mL of protein solution (C_{Stock} = 1.2 mg mL^{-1})

was added and the mixture was stirred overnight at room temperature (0.5 mg BCP per mL Psome + 0.1 mg mL^{-1} protein). Subsequently, the purification was performed by using HFF (1 mM PBS buffer at pH 8, MWCO of 500 kDa, V_{waste} = 150 mL, 150 mbar).

2.3.2. Sequential Approach: i) In Situ Loading of HSA-βCD and Then ii) Post-Functionalization of the Outer Psomes Surface with Avidin/bPEGCOD

HSA-βCD-FITC In Situ Loaded Psomes, Using Psomes C Composition: For in situ loading of HSA-βCD-FITC the method of Gräfe et al. was adopted.[43] 10.5 mg of BCP1 was dissolved in 10.5 mL of 10 mM hydrochloric acid (pH 2) (C_{BCP1} = 1 mg mL^{-1}) and 3 mg BCP2 in 1.5 mL in 10 mM hydrochloric acid (pH 2; 2 mg mL^{-1} pH 2). After complete dissolving and after pass through a 0.2 µm nylon filter for both solutions, 9.8 mL of BCP1 and 1.2 mL of BCP2 were mixed, and 1 mL of HSA-βCD-FITC (1.1 mg mL^{-1}) were added to the freshly prepared BCP solution. Then, the pH was adjusted to pH 9 by adding NaOH slowly. The final block copolymer concentration must be of 1 mg mL^{-1} and the HSA-βCD-FITC concentration of 0.1 mg mL^{-1}. Then, the solution was stirred for 3 days. To receive crosslinked HSA-βCD-FITC in situ loaded Psomes, the solution was placed in the UV-chamber which was irradiated for 180 s. The resulting solution was cleaned from non-enclosed enzyme using HFF. The pH of the Psomes solution was changed into pH 8 then excess amount of β-cyclodextrin in pH 8 PBS buffer (75 µL from β-CD stock solution (10 mg mL^{-1})) was added to displace the HSA-βCD-FITC in the outer surface of Psomes. Again, the mixture was stirred for 2 h then the purification was performed with HFF at pH 8. Two cycles were carried out. Subsequently, the purification of unbounded protein was performed by using HFF (1 mM PBS buffer at pH 8, MWCO of 500 kDa, V_{waste} = 150 mL, 150 mbar).

HSA-Psomes-APEG$_{3kDa}$—Post-Functionalization of HSA-βCD-FITC In Situ Loaded Psomes with Avidin/bPEGCOD$_{3kDa}$ by SPAAC Method: 6 mL of the previous solution (HSA-βCD-FITC in situ loaded Psomes) were added 1 mL of to 1 mM of PBS. The pH was adjusted to pH 8. Then, 2 mL of Avidin/bPEGCOD$_{3kDa}$ solution (1.65 mg) was added and the mixture was stirred overnight at room temperature. Subsequently, the purification of unbounded Avidin/bPEGCOD$_{3kDa}$ was performed by using HFF (1 mM PBS buffer at pH 8, MWCO of 500 kDa, V_{waste} = 150 mL, 150 mbar).

HSA-Psomes-APEG$_{500Da}$—Post-Functionalization of HSA-βCD-FITC In Situ Loaded Psomes with Avidin/bPEGCOD$_{500Da}$ by SPAAC Method: 6 mL of the previous solution (HSA-βCD-FITC in situ loaded Psomes) were added 1 mL of to 1 mM of PBS. The pH was adjusted to pH 8. Then, 2 mL of Avidin/bPEGCOD$_{500Da}$ solution (1.65 mg) was added and the mixture was stirred overnight at room temperature. Subsequently, the purification of unbounded Avidin/bPEGCOD$_{500Da}$ was performed by using HFF (1 mM PBS buffer at pH 8, MWCO of 500 kDa, V_{waste} = 150 mL, 150 mbar).

2.4. Study of Protein-Loaded Psomes by AF4-LS

The vast majority of the samples were analyzed using AF4, the preparation of the samples is described in detail in Supporting Information. All samples were analyzed under the same conditions: 0.25 mg BCP per mL at 1 mM PBS at pH 8.

2.5. Biological Methods

All the experiments with cell cultures were performed in laminar flow work bench Laminair HB2472 (Heraeus Instruments GmbH). Cells were kept in the BBD 6220 CO_2 incubator (Thermo Scientific Heraeus) under constant conditions at 37 °C in 5% CO_2 atmosphere (further details in Supporting Information).

2.5.1. Biocompatibility

The biocompatibility of the structures was validated using the AlamarBlue proliferation assay. HEK293T$_{wt}$ and YTS$_{wt}$ cells were seeded in a 96-well plate at an initial density of 2×10^4 cells per well in 100 µL of complete medium. All compounds were individually evaluated by treating YTS$_{wt}$ and HEK293T$_{wt}$ cells with different concentrations (25–0.1 µg mL^{-1}) of the corresponding samples for 24 h. AlamarBlue reagent (10% v/v) was added to each well and cells were further incubated for 4 h at 37 °C. Finally, the fluorescence intensities were recorded by a microplate reader. 20% dimethyl sulfoxide (Sigma Aldrich) was used as positive control of cellular death. Each experiment was performed by triplicate and the data are shown as the mean value plus standard deviation (SD). Fluorescence intensities in the cytotoxicity experiments were recorded on Synergy 2 Multi Mode Reader (BioTek Instruments) at room temperature (25 °C).

2.5.2. Cellular Uptake Study

Cellular Uptake Study for Different Incubations Times: In order to demonstrate the ability for selective targeting, the Psomes were quantitatively evaluated using flow cytometry analysis. Cells were seeded at density of 2×10^5 cells per well in 1.5 mL of complete medium in a 12-well plate and incubated for 24 h. Then, 60 µL of the corresponding FITC-labeled system (C_F = 0.01 mg mL^{-1}, stock solution in PBS) were added, the cells were incubated at 37 °C in a humidified 5% CO_2 incubator for different incubation times (0, 4, and 24 h). After desired incubation time, cells were washed with PBS and 0.1% heparin (in order to remove compounds that were attached on the surface but not internalized) followed by centrifugation at 300 × *g* for 5 min at 4 °C. The resulting pellets were suspended in 200 µL PBS and analyzed by flow cytometry.

Inhibition with Neutravidin: In order to demonstrate the ability for selective targeting, an inhibition experiment with neutravidin was carried out. HEK293T$_{huBirA\text{-}DAP12\text{-}KiBAP}$ (at density of 2×10^5 cells per well in 1.5 mL of complete medium) were seeded in a 12-well plate and incubated for 24 h. Next, the medium was removed, and 1.5 mL of new medium (without FBS) was added. Later, the cells were treated with 0.01 mg mL^{-1} of neutravidin and incubated for 30 min. Afterward, 60 µL of the corresponding FITC-labeled system (C_F = 0.01 mg mL^{-1}, stock solution in PBS) were added, the cells were incubated at 37 °C in a humidified 5% CO_2 incubator for different incubation times (0, 2, 4, and 6 h).

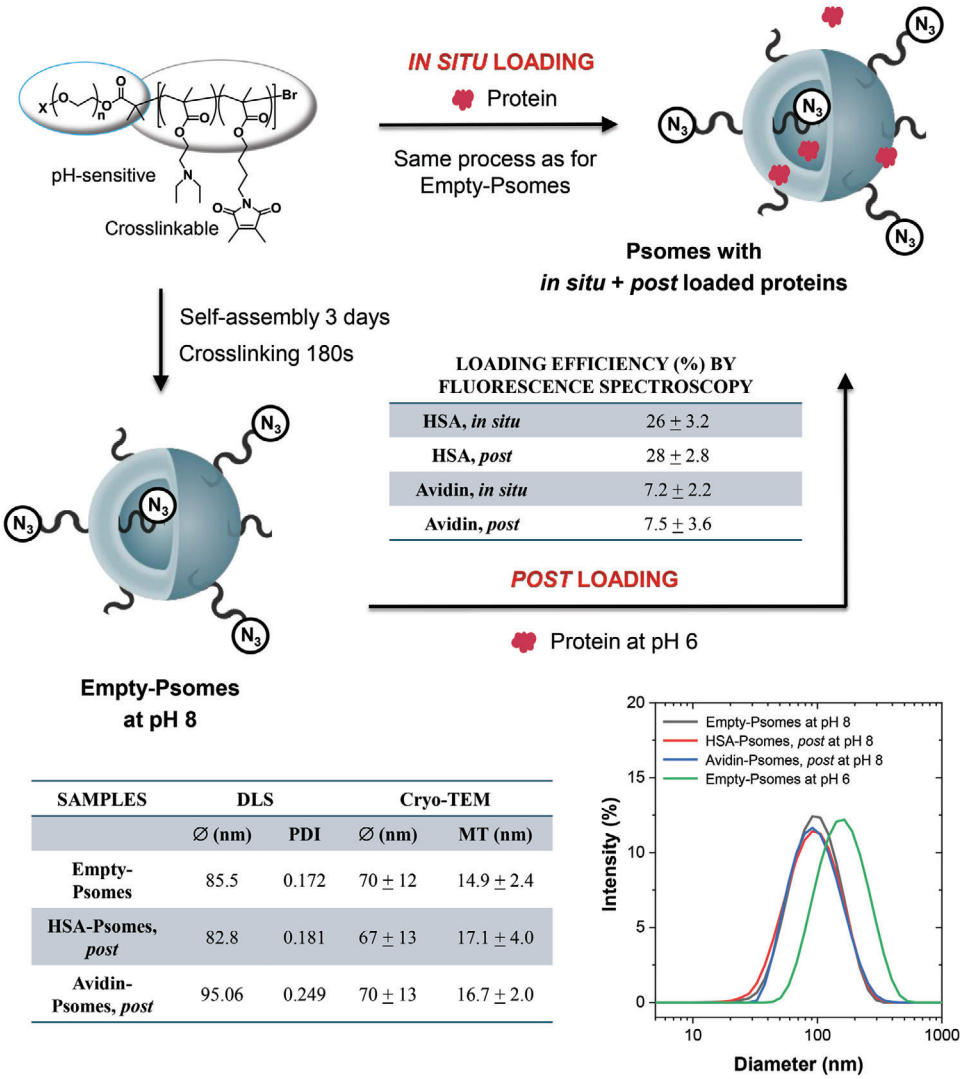

SAMPLES	DLS		Cryo-TEM	
	∅ (nm)	PDI	∅ (nm)	MT (nm)
Empty-Psomes	85.5	0.172	70 ± 12	14.9 ± 2.4
HSA-Psomes, *post*	82.8	0.181	67 ± 13	17.1 ± 4.0
Avidin-Psomes, *post*	95.06	0.249	70 ± 13	16.7 ± 2.0

Figure 2. General approach for preparing protein-loaded polymersomes (Psomes). Conditions: 1 mg BCP per mL + 0.1 mg mL^{-1} protein. Characterization by fluorescence spectroscopy (HSA-FITC or Avidin/bPEGFITC), DLS, and Cryo-TEM. Psomes C composition [80% BCP1 (X = methoxy end group) + 20% BCP2 (X = azido end group)] used for preparing protein in situ and post loaded Psomes. ∅ = diameter. MT = membrane thickness. The % loading efficiency was calculated by fluorescence intensity after purification divided by fluorescence intensity before purification.

After desired incubation time, cells were washed with PBS and 0.1% heparin followed by centrifugation at 300 × *g* for 5 min at 4 °C. The resulting pellets were suspended in 200 µL PBS and analyzed by flow cytometry.

2.6. Statistical Analysis and Figures

The main figures were represented using Origin 2016 software. The statistical analysis, including the calculation of the mean, standard deviation, and *p*-values, was performed using the Mann–Whitney U nonparametric test. The significance level was set as $p \leq 0.05$. GraphPad Prism 5.0 software was used. All data were generated from duplicate or triplicate wells in at least three independent experiments.

3. Results and Discussion

3.1. Formation and Characterization of Azido-Modified-Psomes

pH-responsive and photo-crosslinked Psomes decorated with azide groups were prepared by mixed self-assembly of methoxy- and azido-modified block copolymers (**Figure 2**).[15,51] The corresponding block copolymers (BCP1 and BCP2, Figure 2) were synthesized by atom transfer radical polymerization using a previously published approach.[51,52] Both block copolymers are characterized by a methoxy end group (BCP1) or a azide end group (BCP2) in the hydrophilic poly(ethylene glycol) (PEG) segment, while their hydrophobic part consists of pH-sensitive 2-(*N*,*N*′-diethylamino)ethyl methacrylate (DEAEM) and photo-crosslinker, 3,4-dimethyl maleic imidobutyl methacrylate. The Psomes were fabricated by the self-assembly of different

mixtures of BCP1 and BCP2 (Psomes A = 100% BCP1; Psomes B = 90% BCP1 + 10% BCP2, and Psomes C = 80% BCP1 + 20% BCP2) using the so-called pH switch method.[51,52] Afterward Psomes were crosslinked by UV irradiation for 180 s. The obtained Psomes A-C were characterized by DLS (size, polydispersity, and swelling-shrinking cycles of vesicles). The average size of Psomes A-C at pH = 8 is around 85–95 nm, while at pH = 5 the average size of them is around 135–160 nm depending of the percentage of BCP2 (Table S3, Supporting Information). Due to the photo-crosslinking process Psomes A–C exhibit the desired enhanced mechanical stability and repeated swelling and shrinking of Psomes membrane even in a high number of pH cycles (Figure S8, Supporting Information) as known from previous studies.[65] To investigate the controlled post-functionalization of azido-modified Psomes by SPAAC, Psomes C with the highest azido block copolymer percentage (20% N_3) was chosen for the following studies, because of the presence of enough azido groups on the exterior surface of Psomes.[51] Previously, our pH-responsive Psomes were thoroughly studied by AF4-LS, leading to a better understanding of scaling parameters (e.g., shape and density).[65] Therefore, the influence of the incorporation of BCP2 in azido-modified Psomes on the scaling parameter was studied by AF4-LS using different percentages of BCP2 (0%, 5%, 10%, and 20% N_3) (Figure S10, Supporting Information, top). The resulting scaling parameter ν (0.39–0.43) at different BCP2 ratios is quite similar, showing a conformation close to a spherical shape (ideal sphere $\nu = 0.33$). Considering the apparent density of all Psomes in Figure S10, Supporting Information (middle), the apparent density significantly drops at the highest percentage (20% N_3), due to increase of R_g for Psomes with 20% N_3 (Figure S10, Supporting Information, middle). In addition, the ρ parameters (R_g/R_h) were determined to be 1.1–1.4 (Figure S10, Supporting Information, bottom). The highest value (1.4) was found for the highest percentage (20% N_3) corresponding to a more heterogeneous particle surface for Psomes with 20% N_3 (Psomes C composition). This might be due to the high amount of BCP2 in Psomes which contains a longer PEG chain compared to BCP1, leading to a more irregular surface and deviation of ρ parameters from the ideal value for hollow capsules ($\rho = 1$).

3.2. Formation and Characterization of Protein-Loaded Psomes Using Post and In Situ Loading Approaches

The first study was to investigate the loading efficiency of these Psomes of two proteins such as avidin and HSA by in situ (during the formation) and post (after formation at acidic pH) loading (Figure 2). Both proteins possess similar sizes (≈66 kDa) but an opposite surface charge under the conditions studied (range pH 6–8; HSA (pI = 4.9, negative charge); Avidin (pI = 10, positive charge)). Additionally, both proteins present different hydrophilic/hydrophobic character. Avidin presents a more hydrophilic character than HSA due to a higher percentage of polar amino acids (≈60%) and also the presence of carbohydrates at the protein surface. This difference could highly contribute to the interaction with the Psomes, but also to the location and loading efficiency of both proteins. Previous studies demonstrated that in situ loading of enzymes into our Psomes is useful to construct nanoreactors with "on and off"-switchable enzymatic cascade reactions.[43,44,46] Further studies extended these results to the post loading approach.[65,66] For both loading approaches, the same amount of proteins was used (1 mg BCP per mL + 0.1 mg mL^{-1} protein). Successful loading by the Psomes was proven by fluorescence spectroscopy using labeled proteins (HSA-FITC or Avidin/bFITC, Supporting Information). Free protein within the protein-loaded Psomes (HSA-Psomes and Avidin-Psomes) solution was removed by hollow fiber filtration (HFF) purification (Figure 2). By fluorescence spectroscopy, a large difference in the loading efficiency for the two proteins is observed (HSA ≈26%, Avidin ≈8%). However, the difference in loading efficiency is negligible, when considering the loading method for each protein (Figure 2). Without doubt, the large loading difference of both proteins is attributed to the opposite surface charge, and hydrophilic/hydrophobic character, favoring the interaction of HSA with the positively charged surface of the Psomes at acidic pH and hydrophobic membrane interaction at basic pH.

Regarding the loading by the two different loading methods, the cargo location depending on the type of cargo has also to be considered, even though the loading efficiency was the same. Using in situ loading, the protein will be mainly found inside and anchored in the membrane.[46,66] Using post loading, the membrane and surface of Psomes will be more favored.[50,65] Thus, the choice of loading approach will depend on the subsequent application of those protein-loaded Psomes desired.[43,44,65,66] Furthermore, the presence of proteins in HSA-Psomes and Avidin-Psomes results in slightly larger membrane thicknesses compared to the reference, Empty-Psomes (Figure 2). This is similar to results found in other studies with membrane-integrated enzymes in Psomes.[65,66]

To validate the aforementioned possible locations of proteins in HSA-Psomes and Avidin-Psomes, once more an in-depth characterization by AF4-LS was carried out (**Figure 3**). For this AF4-LS study, no purification step was performed to in situ and post loading solutions; thus, free protein and Protein-Psomes were coexisting in the sample solution (Figure S13, Supporting Information). AF4-LS conditions are 0.25 mg BCP per mL with/without 0.025 mg mL^{-1} protein in 1 mM PBS at pH 8 (further details about the fabrication of Protein-Psomes and Empty-Psomes are in the Supporting Information).

The resulting scaling parameters ν show spherical shape for all Protein-Psomes with very tiny differences ($\nu = 0.3$–0.4). Similar structural parameters to previous studies with Avidin-Psomes without azide groups were found. The corresponding apparent density of Protein-Psomes drops significantly in all cases except for Avidin-Psomes-in situ. The high apparent density of Avidin-Psomes-in situ can be explained that in this case with i) the more favored lumen than the membrane location of avidin or ii) lower loading efficiency surface in comparison with the rest of the samples. This affects the R_g too, leading to smaller R_g (Figure 3).

Moreover, the ρ parameters (R_g/R_h) were determined (Figure 3; Table S5, Supporting Information). The value of Avidin-Psomes-post (0.83) corresponds to a state which can be described as hard sphere-like conformation differently (Figure 3, bottom right) than for Empty-Psomes (0.99). Based on previous studies, post loaded avidin cannot cross the membrane due to its size.[66] This leads to the conclusion, that different membrane locations are preferred by avidin giving different segments for R_g and causing the observed ρ parameters changes. However, all

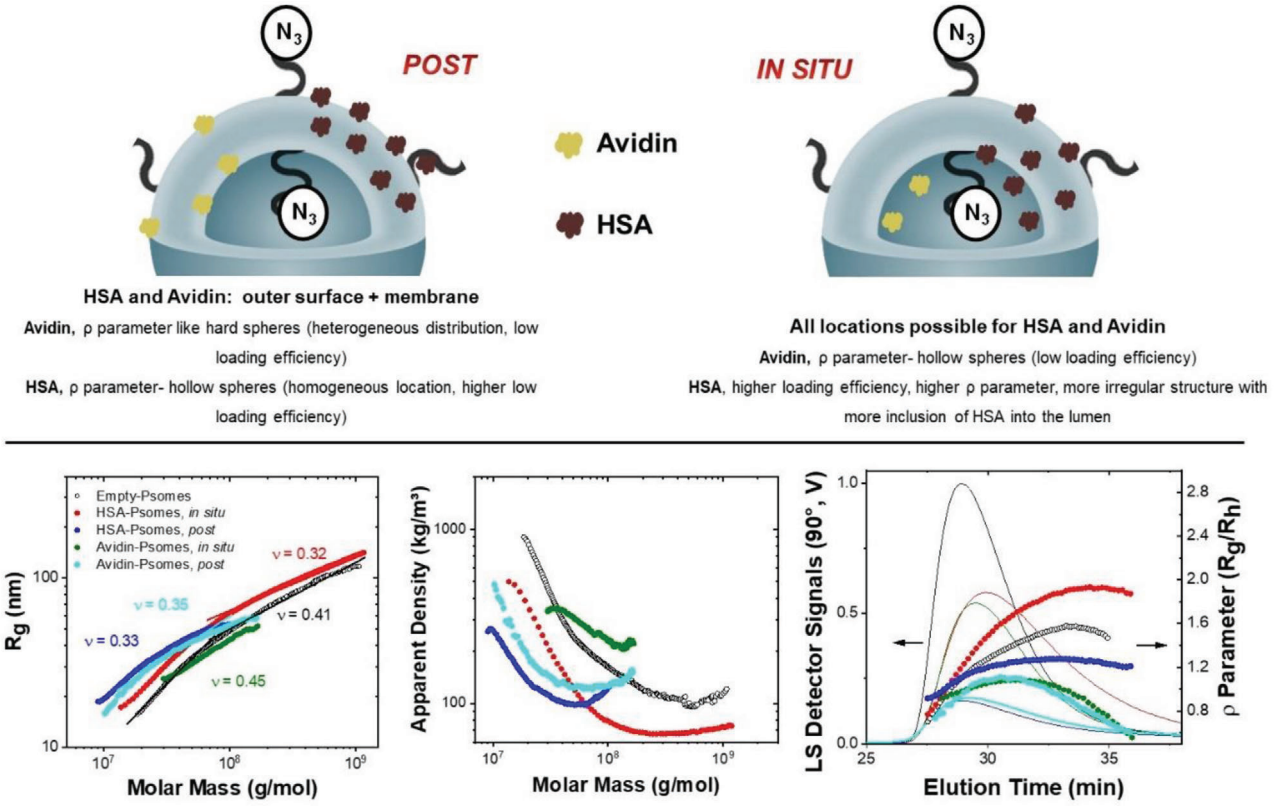

Figure 3. AF4 conformation studies: (Top) Postulation of avidin and HSA's locations after each used loading method. (Bottom-left) Conformation plot of polymersomes (Psomes) measured at pH 8. (Bottom-middle) Determination of the apparent density calculated according to molar mass and radius (R_g). (Bottom-right) LS signal and ρ-parameter (R_g/R_h) versus elution time. Conditions: 0.25 mg BCP per mL + 0.025 mg mL^{-1} avidin or HSA. Apparent density calculated for Psomes: Empty and in situ and post loaded with protein. Using Psomes C composition (80% BCP1 + 20% BCP2) for preparing protein in situ and post loaded Psomes. Equations for the determination of different parameters by AF4-LS presented in Supporting Information.

parameters are very similar to Empty-Psomes for Avidin-Psomes-in situ (0.99). Thus, in combination with other studies, avidin is mainly found in the lumen, in the hydrophilic part, but due to the low level of efficiency, the ρ parameter is similar to Empty-Psomes. The different protein-filling scenarios of both samples are additionally supported by the observed density trends.

At the same time, the ρ value in the case of HSA-Psomes-post indicates a hollow sphere shape for the post loaded sample. This allows us to postulate that the HSA post location is focused in the membrane or on the surface of the Psomes, corroborating again that the HSA prefers the hydrophobic region. In contrast, HSA-Psomes-in situ sample shows higher ρ parameter corresponding to more irregular structure with inclusion of HSA into the lumen (high density at low molar masses) with the tendency to aggregation to some extent, also confirmed by the decreasing density at higher molar masses.

The most surprising results within the AF4-LS study are the different ρ values for HSA-Psomes-post and Avidin-Psomes-post, when starting from the same Empty-Psomes. This implies a different protein-filling state for both post loaded Psomes (Figure 3, top left). The different behavior may be the combination of different parameters such as: a) the opposite surface charge, b) the different hydrophobic/hydrophilic balance, and c) the presence of azide groups and heterogeneous inner and outer PEG shells generating additional interactions as well.

In contrast to the high shear-force applied during HFF,[66,67] the forces applied during AF4 separation are too weak to break the interaction between the vesicle surface and the cargo. Unfortunately, a direct quantification of loaded avidin is not possible due to some interaction with the membrane in the AF4-channel (low mass recovery, Table S4, Supporting Information). In contrast, a separation and quantification in the case of HSA is possible. The correlation of the UV signal areas varied with concentration series of the individual proteins enables us to quantify the free protein and to calculate the amount of loaded protein in the Psomes (Figures S12, S13, Table S5, Supporting Information). Using this well-established protocol,[66,68] a corrected loading efficiency of 31% for HSA in situ (22 Protein:Psomes) and 42% for HSA post loading (30 Protein:Psomes). It can be observed that the values are higher from those listed in the table in Figure 2 (26% for HSA in situ and 28% for HSA post, purified by HFF), which is a result of the high shearing forces applied by HFF in comparison to AF4 as discussed above. Based on the AF4 results without the use of high shear forces, a higher number of HSA biomacromolecules is loaded using post loading. Thus, it might be that using this strategy preferred electrostatic interactions are promoted raising the loading efficiency, which provides a valuable information for other bio(macro)molecules. For instance, in case a protein release is necessary for a therapeutic action, a post loading approach would be more efficient

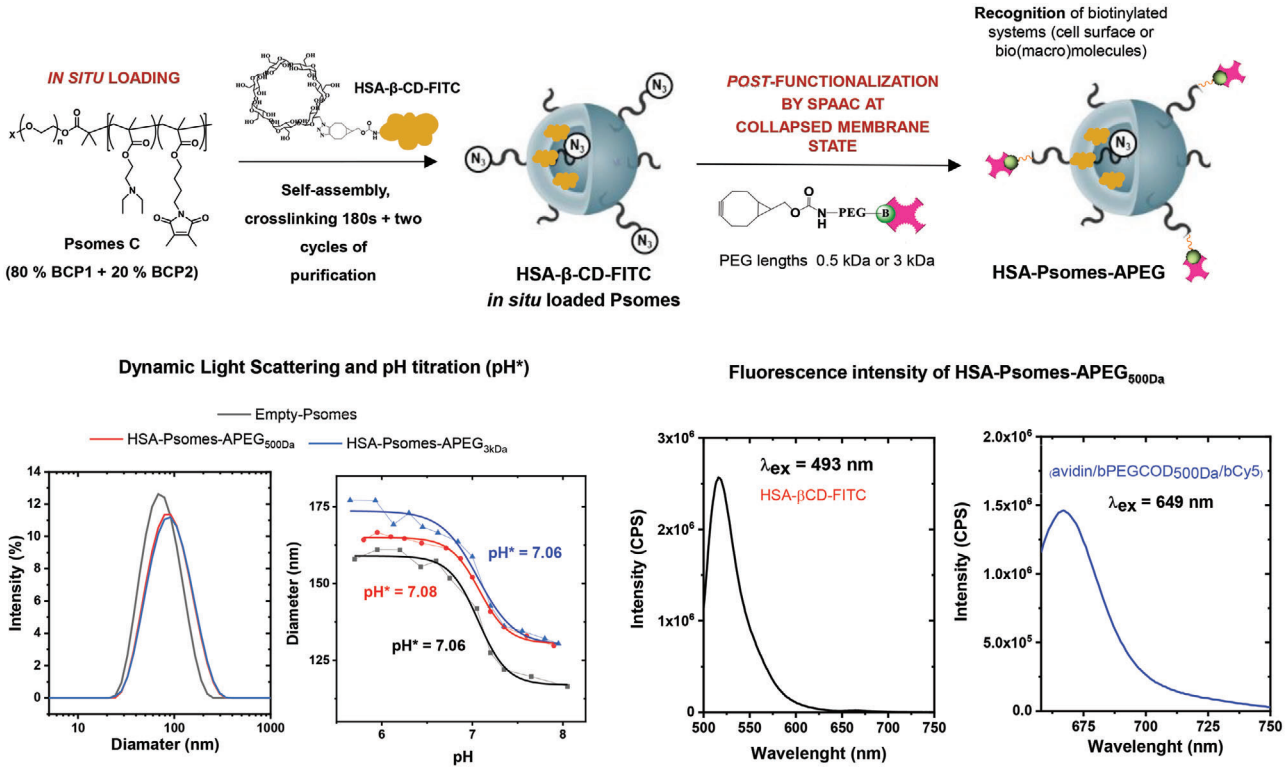

Figure 4. (Top) Fabrication of HSA in situ loaded and avidin post-functionalized polymersomes, HSA-Psomes-APEG$_{500Da}$, and HSA-Psomes-APEG$_{3kDa}$ (HSA-Psomes-APEG). First step, in situ loading: 1 mg BCP per mL + 0.2 mg mL^{-1} HSA-β-CD-FITC. The HSA on the surface is displaced by excess of β-CD. Second step, post-functionalization: 0.25 mg BCP per mL + 0.1 mg mL^{-1} Avidin/bPEG$_{3kDa/500Da}$COD. (Bottom) Characterization of HSA in situ loaded and avidin post-functionalized polymersomes. pH-dependent DLS measurements determination of pH* (half-power of Psomes swelling) of protein-loaded Psomes (0.25 mg BCP per mL in 1 mM PBS). Monitoring the sequential approach by fluorescence intensity.

for biomacromolecules with properties (charge and size) similar to HSA.

3.3. Post-Functionalization Reactions on the Psomes with Surface-Modified HSA

Next step was the post-functionalization on the Psomes surface in the state of collapsed membrane (**Figure 4**) by applying SPAAC reaction using the azide groups on the Psomes surface and cyclooctyne-(COD)-modified HSA protein and to compare this post-functionalization with the unspecific interactions between β-CD groups and PEG chains in the case of HSA-β-CD. Therefore, surface-modified proteins such as HSA-COD and HSA-β-CD and their labeled analogues were prepared and characterized (details in the Supporting Information).[68] To avoid aggregation processes under SPAAC and non-covalent interaction conditions, the reaction between N_3-modified Psomes and surface-modified HSA was carried out under dilute conditions (0.25 mg mL^{-1} of Psomes) and at pH 8 to ensure the desired post-functionalization on Psomes surface. The reaction mixture was stirred overnight and the resulting post-functionalized Psomes were purified by HFF and characterized by UV–vis and fluorescence spectroscopy (Figures S14, S15, Supporting Information).

First, non-specific interactions (Figure S15, Supporting Information) are observed in the case of HSA-β-CD (≈30%), but a higher functionalization is obtained in the case of HSA-COD (≈50%) without aggregation processes (details in Supporting Information). Over time the HSA post-modified Psomes showed a small amount of aggregation once they are stored at 4 °C for several days. However, these specific dye-labeled HSA post-functionalized Psomes could not be used for cellular uptake study. They resulted in very high, non-specific cellular uptakes (data not shown), due to the presence of high number of FITC groups of HSA on the Psomes´ surface. Therefore, these samples were discarded for further biological studies. Though, the study showed that the combination of a protein loading of Psomes with a protein post-functionalization process for the fabrication of a potential drug delivery system can be in principle achieved. The final post-functionalization on Psomes surface with collapsed membrane at pH 8 avoids the loading of any proteins in the lumen or in the Psomes membrane as known from post loading processes.[65]

3.4. HSA-Loaded Psomes with Avidin as Recognition Unit at the Outer Psomes Surface for a First Molecular Recognition Study

The second method consisted of a sequential approach (Figure 4): i) in situ loading of HSA-β-CD-FITC and then ii) post-functionalization of the outer Psomes´ surface with avidin/bPEGCOD using different PEG spacers (500 Da

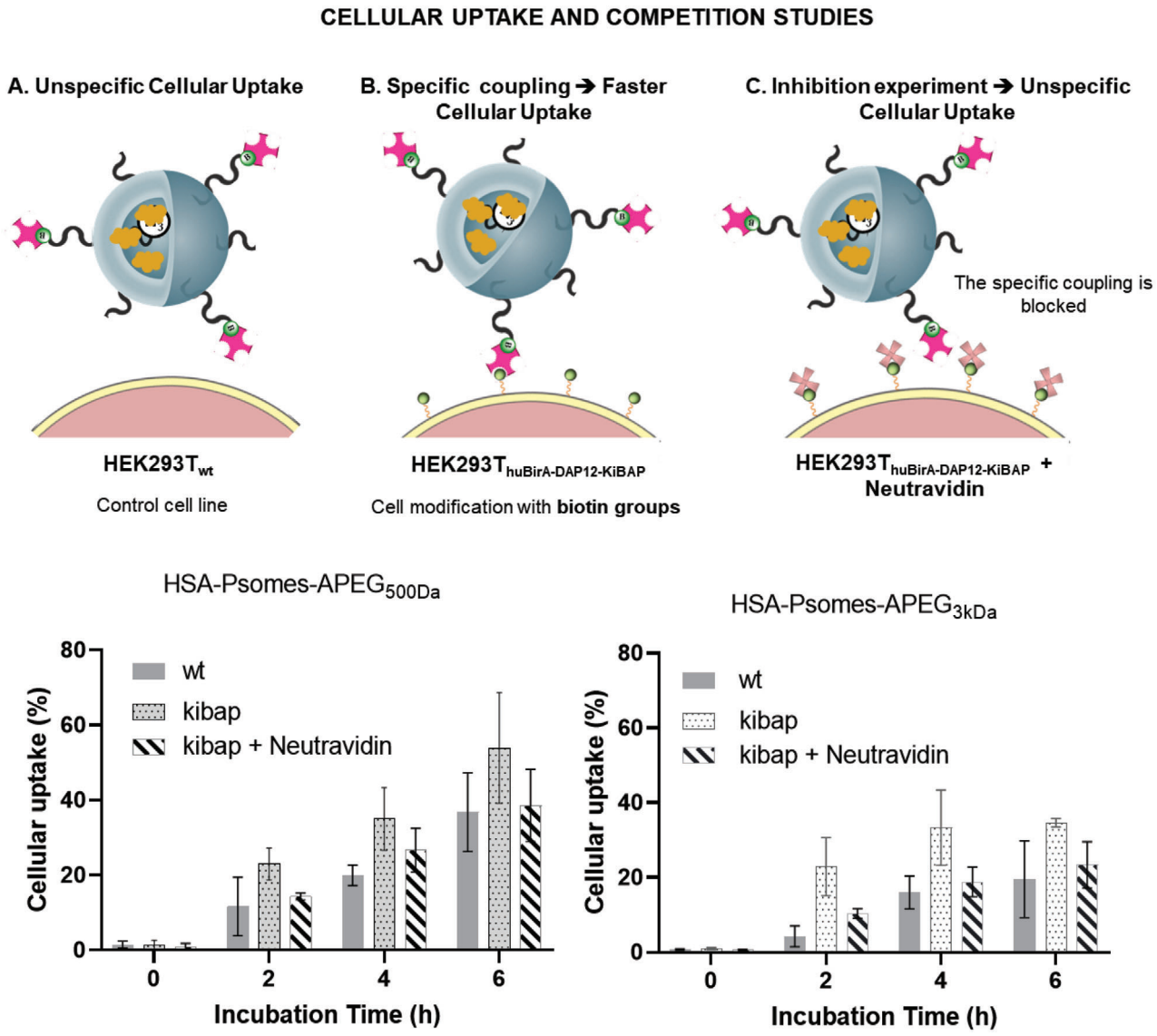

Figure 5. Cellular uptake and competition studies of protein in situ loaded and post-functionalized Psomes, HSA-Psomes-APEG$_{500Da}$, and HSA-Psomes-APEG$_{3kDa}$ (10 μg BCP per mL). A. HEK293T$_{wt}$ cell line was used as negative control; B. HEK293T$_{huBirA-DAP12-KiBAP}$ cell line was used to prove the successful interaction between Avidin post-modified Psomes nanoobjects and biotinylated cell surface receptor; C. HEK293T$_{huBirA-DAP12-KiBAP}$ cell line in presence of neutravidin was used for competition studies.

(PEG$_{500Da}$) and 3000 Da (PEG$_{3kDa}$)) (details on the synthesis and characterization in Supporting Information). Post-functionalization of Psomes surface with avidin/bPEGCOD was carried out under the same experimental conditions of SPAAC as described above for HSA post-modified Psomes. The polymeric vesicles were characterized by DLS and zeta-potential (Figure 4; Figure S16, Supporting Information), and the post-functionalization and purification processes were monitored by fluorescence spectroscopy indicating the successful loading of HSA-β-CD-FITC, preferentially located in the lumen of Psomes, and the successful post-functionalization of avidin/bPEGCOD on the Psomes surface (Figure 4).

Due to the high loading efficiency of HSA by in situ loading (Figure 2) and presence of some HSA biomacromolecules on Psomes´ surface, as mentioned above, it is very important to remove the HSA-β-CD-FITC from the surface for subsequent cellular uptake experiments. To do this, two cycles of treatment with excess β-CD were carried out to displace the HSA-β-CD-FITC on the surface obtaining the desired system (Figure S9, Supporting Information) before carrying out final post-functionalization of Psomes-loaded HSA-β-CD-FITC (HSA-Psomes; Figure 4). With the fabrication of avidin/bPEG$_{500Da}$COD and avidin/bPEG$_{3kDa}$COD post-modified HSA-Psomes (HSA-Psomes-APEG$_{500Da}$ and HSA-Psomes-APEG$_{3kDa}$), we were able to validate their first recognition potential through biotin ligand-carrying cell surfaces (**Figure 5**). Previously, we evaluated the tendency for particle aggregation/stability of Empty-Psomes and protein-loaded Psomes in different cell media. Briefly,

Empty-Psomes (0.25 mg BCP per mL), HSA-Psomes (0.25 mg BCP per mL) and HSA-Psomes-Avidin (0.125 mg BCP per mL) were incubated at 37 °C in three different solutions: a) 1 mM PBS, b) serum-free DMEM, and c) 10% FBS DMEM. All samples were analyzed by DLS after different time points of incubation (0, 2, 4, 6, and 24 h). The results are shown in the Table S6 and Figure S17, Supporting Information. This strategy could be extended to a therapeutic protein/enzyme with properties similar to HSA, which could be activated or released under specific conditions, combined with targeting properties.

3.5. In-Vitro Study

For biological approaches protein-loaded nanocarriers need to be nontoxic, non-immunogenic, and biocompatible.[69] To study Psomes biocompatibility, human embryonic kidney carcinoma cell line (HEK293T$_{wt}$) and NK-cell leukemia cell line (YTS$_{wt}$; Table S6, Supporting Information) were treated for 24 h with different concentrations of HSA-Psomes-APEG$_{500Da}$ or HSA-Psomes-APEG$_{3kDa}$ (0.1–25 μg mL^{-1}). As shown in Figure S18, Supporting Information both Psomes exhibit similar toxicities. The maximum nontoxic concentration in YTS$_{wt}$ is 25 μg mL^{-1} compared to 10 μg mL^{-1} in HEK293T$_{wt}$. This difference can be attributed to the different characteristics of the cell lines. To avoid toxicity, a concentration of 10 μg mL^{-1} of HSA-Psomes-APEG$_{500Da}$ or HSA-Psomes-APEG$_{3kDa}$ was used for further studies.

Next, we analyzed specific uptake of avidin post-functionalized HSA-Psomes into biotinylated target cells. Therefore YTS$_{huBirA\text{-}DAP12\text{-}KiBAP}$ and HEK293T$_{huBirA\text{-}DAP12\text{-}KiBAP}$, expressing biotinylated DAP12 receptor on their cell surface were incubated with 60 μL of PBS containing the corresponding FITC-labeled HSA-Psomes-APEG systems (C_F = 0.01 mg mL^{-1}) at 37 °C for different incubation times (0, 4, and 24 h). As negative control, HEK293T$_{wt}$ and YTS$_{wt}$ were used. After different incubation times, cells were washed with PBS and 0.1% heparin in order to remove HSA-Psomes-APEG$_{500Da}$ and HSA-Psomes-APEG$_{3kDa}$ that are attached on the cell surface. The resulting pellets were suspended in 200 μL PBS and analyzed by flow cytometry (Figure 5; Figure S20, Supporting Information).

As depicted in Figure S22, Supporting Information HSA-Psomes-APEG$_{500Da}$ are internalized independently of the biotinylated surface receptor in YTS cell lines after 24 h incubation time. In comparison HSA-Psomes-APEG$_{500Da}$ are internalized specifically by biotinylated DAP12 expressing HEK293T cells. The specific uptake is even detectable after 24 h. However, HEK293T$_{wt}$, that do not express biotinylated DAP12 receptor on their cell surface, also internalizes HSA-Psomes-APEG$_{500Da}$ non-specifically to some extent. In addition, we performed a competition assay to analyze whether specific cellular uptake of avidin post-functionalized HSA-Psomes can be inhibited by blocking biotinylated cell surface receptors with neutravidin. Therefore, HEK293T$_{huBirA\text{-}DAP12\text{-}KiBAP}$ was treated with HSA-Psomes-APEG$_{500Da}$ or HSA-Psomes-APEG$_{3kDa}$ in presence and absence of neutravidin. Hek293T$_{wt}$ served as negative control (Figure 5).

As shown Figure 5, both HSA-Psomes-APEG$_{500Da}$ and HSA-Psomes-APEG$_{3kDa}$ are specifically internalized by HEK293T$_{huBirA\text{-}DAP12\text{-}KiBAP,}$ expressing biotinylated DAP12 receptor on their cell surface. In comparison, blocking the receptor with neutravidin inhibits the specific uptake of HSA-Psomes-APEG$_{500Da}$ and HSA-Psomes-APEG$_{3kDa}$ by HEK293T$_{huBirA\text{-}DAP12\text{-}KiBAP}$ cells. In the presence of neutravidin, cellular uptake is comparable to the non-specific internalization of HSA-Psomes-APEG$_{500Da}$ and HSA-Psomes-APEG3$_{kDa}$ by HEK293T$_{wt}$, which do not express a biotinylated receptor on their cell surface. These results indicate that avidin post-functionalized HSA-Psomes are an attractive targeted drug delivery system, regardless of the length of the PEG chain used. The described protein in situ loaded and post-functionalized Psomes possess the capability to bind specifically biotinylated receptors on the cell surface of cancer cells. Moreover, they can be specifically internalized by these cells. To further improve specific cellular uptake and reduce unspecific cell binding of our Psomes biohybrids, it might be better to combine the concept of freely dangling targeting ligand with neutravidin on Psomes´ surface. Compared to avidin, neutravidin is free of sugar units and has a neutral isoelectric point, which minimizes non-specific binding to cell membranes.[70]

4. Conclusion

This study provides deeper insights into the establishment of multiple protein-loaded Psomes based on the use of pH-responsive and azido-modified Psomes with the focus on the structural characterization and loading and post-functionalization possibilities. The following issues were evaluated: a) different loading processes (in situ and post) with their corresponding loading efficiency; b) two types of proteins for loading with similar size but different surface charge and polarity (HSA and avidin); c) structural parameters of azido-modified Psomes in the presence and absence of loaded proteins; and d) the ability of Psomes as selective recognition systems using SPAAC for post-functionalization on Psomes surface. The consideration of the structural parameters (Figure 3) and cryo-TEM results (Figure 2) allowed us to suggest different potential protein locations in Protein-Psomes (Figure 3, top).

It has to be emphasized that the present work differs strongly from recently published results that describe the docking and diffusion processes of biotinylated cargo on/in Avidin-Psomes, prepared by in situ loading and avidin-biotin conjugation process.[66] Moreover, matrix metalloproteinase-1 post loaded Psomes with PEG shell outline promising benefits for the treatment of early liver fibrosis, leading to the degradation of extracellular collagen-1.[50] Our azido-modified, biocompatible, and pH-responsive azido-modified Psomes, post-functionalized, and/or loaded with proteins/enzymes, can be further post-functionalized with other bio(macro)molecules such as antibodies, peptides, or enzymes by click chemistry or by biotin-avidin (derivative) interaction. The current work paves the way to the fabrication of nanocompartments with multiple functions, while the location of active bio(macro)molecules will be selected and determined by its therapeutic action, size, and polarity. The highly versatile azido-modified Psomes system offers new opportunities for the design of targeting protein therapeutics, targeting therapeutics nanoreactors, and as diverse cell biomimetics.

Supporting Information

Supporting Information is available from the Wiley Online Library or from the author.

Acknowledgements

The authors gratefully acknowledge Dr. Petr Formanek for performing Cryo-TEM measurements, Christina Harnisch for carrying out SEC measurements, and Katja Robel for the excellent maintenance of cell lines.

Open access funding enabled and organized by Projekt DEAL.

Conflict of Interest

The authors declare no conflict of interest.

Data Availability Statement

Data available on request due to privacy/ethical restrictions

Keywords

in situ and post loading, molecular recognition and conjugation, polymersomes, post-functionalization, proteins, SPAAC

Received: March 14, 2021
Revised: July 22, 2021
Published online: August 6, 2021

[1] S. Hossen, M. K. Hossain, M. K. Basher, M. N. H. Mia, M. T. Rahman, M. J. Uddin, *J. Adv. Res.* **2019**, *15*, 1.
[2] S. Iqbal, M. Blenner, A. Alexander-Bryant, J. Larsen, *Biomacromolecules* **2020**, *21*, 1327.
[3] O. Onaca, R. Enea, D. W. Hughes, W. Meier, *Macromol. Biosci.* **2009**, *9*, 129.
[4] L. Messager, J. R. Burns, J. Kim, D. Cecchin, J. Hindley, A. L. Pyne, J. Gaitzsch, G. Battaglia, S. Howorka, *Angew. Chem., Int. Ed.* **2016**, *55*, 11106.
[5] J. Sun, M. Mathesh, W. Li, D. A. Wilson, *ACS Nano* **2019**, *13*, 10191.
[6] Y. Tu, F. Peng, X. Sui, Y. Men, P. B. White, J. C. M. van Hest, D. A. Wilson, *Nat. Chem.* **2017**, *9*, 480.
[7] H. Che, J. C. M. van Hest, *J. Mater. Chem.* **2016**, *4*, 4632.
[8] X. Hu, Y. Zhang, Z. Xie, X. Jing, A. Bellotti, Z. Gu, *Biomacromolecules* **2017**, *18*, 649.
[9] U. Kauscher, M. N. Holme, M. Björnmalm, M. M. Stevens, *Adv. Drug Delivery Rev.* **2019**, *138*, 259.
[10] P. V. Pawar, S. V. Gohil, J. P. Jain, N. Kumar, *Polym. Chem.* **2013**, *4*, 3160.
[11] R. J. R. W. Peters, M. Marguet, S. Marais, M. W. Fraaije, J. C. M. van Hest, S. Lecommandoux, *Angew. Chem., Int. Ed.* **2014**, *53*, 146.
[12] H. Bäumler, R. Georgieva, *Biomacromolecules* **2010**, *11*, 1480.
[13] M. Li, X. Huang, T. Y. Tang, S. Mann, *Curr. Opin. Chem. Biol.* **2014**, *22*, 1.
[14] M. Marguet, C. Bonduelle, S. Lecommandoux, *Chem. Soc. Rev.* **2013**, *42*, 512.
[15] M. A. Yassin, D. Appelhans, R. Wiedemuth, P. Formanek, S. Boye, A. Lederer, A. Temme, B. Voit, *Small* **2015**, *11*, 1580.
[16] S. Jia, W.-K. Fong, B. Graham, B. J. Boyd, *Chem. Mater.* **2018**, *30*, 2873.
[17] J. Leong, J. Y. Teo, V. K. Aakalu, Y. Y. Yang, H. Kong, *Adv. Healthcare Mater.* **2018**, *7*, 1701276.
[18] T. O. Pangburn, F. S. Bates, E. Kokkoli, *Soft Matter* **2012**, *8*, 4449.
[19] T. O. Pangburn, K. Georgiou, F. S. Bates, E. Kokkoli, *Langmuir* **2012**, *28*, 12816.
[20] T. Thambi, J. H. Park, D. S. Lee, *Biomater. Sci.* **2016**, *4*, 55.
[21] S. Egli, H. Schlaad, N. Bruns, W. Meier, *Polymers* **2011**, *3*, 252.
[22] C. Zelmer, L. P. Zweifel, L. E. Kapinos, I. Craciun, Z. P. Güven, C. G. Palivan, R. Y. H. Lim, *Proc. Natl. Acad. Sci. U. S. A.* **2020**, *117*, 2770.
[23] J. K. Patra, G. Das, L. F. Fraceto, E. V. R. Campos, M. d. P. Rodriguez-Torres, L. S. Acosta-Torres, L. A. Diaz-Torres, R. Grillo, M. K. Swamy, S. Sharma, S. Habtemariam, H.-S. Shin, *J. Nanobiotechnol.* **2018**, *16*, 71.
[24] S. A. Meeuwissen, M. F. Debets, J. C. M. van Hest, *Polym. Chem.* **2012**, *3*, 1783.
[25] S. J. Rijpkema, B. J. Toebes, M. N. Maas, N. R. M. de Kler, D. A. Wilson, *Isr. J. Chem.* **2019**, *59*, 928.
[26] D. Park, C. Lee, M. Chae, M. A. Kadir, J. E. Choi, J. K. Song, H.-J. Paik, *Polymers* **2017**, *9*, 144.
[27] K. Yoshida, S. Tanaka, T. Yamamoto, K. Tajima, R. Borsali, T. Isono, T. Satoh, *Macromolecules* **2018**, *51*, 8870.
[28] S. Egli, M. G. Nussbaumer, V. Balasubramanian, M. Chami, N. Bruns, C. Palivan, W. Meier, *J. Am. Chem. Soc.* **2011**, *133*, 4476.
[29] A. L. Martin, B. Li, E. R. Gillies, *J. Am. Chem. Soc.* **2009**, *131*, 734.
[30] S. J. Rijpkema, S. G. H. A. Langens, M. R. van der Kolk, K. Gavriel, B. J. Toebes, D. A. Wilson, *Biomacromolecules* **2020**, *21*, 1853.
[31] M. A. Bruckman, G. Kaur, L. A. Lee, F. Xie, J. Sepulveda, R. Breitenkamp, X. Zhang, M. Joralemon, T. P. Russell, T. Emrick, Q. Wang, *ChemBioChem* **2008**, *9*, 519.
[32] N. Li, W. H. Binder, *J. Mater. Chem.* **2011**, *21*, 16717.
[33] J. A. Opsteen, R. P. Brinkhuis, R. L. M. Teeuwen, D. W. P. M. Lowik, J. C. M. van Hest, *Chem. Commun.* **2007**, 3136.
[34] P. Thirumurugan, D. Matosiuk, K. Jozwiak, *Chem. Rev.* **2013**, *113*, 4905.
[35] D. P. Nair, M. Podgórski, S. Chatani, T. Gong, W. Xi, C. R. Fenoli, C. N. Bowman, *Chem. Mater.* **2014**, *26*, 724.
[36] M. Gutmann, E. Memmel, A. C. Braun, J. Seibel, L. Meinel, T. Lühmann, *ChemBioChem* **2016**, *17*, 866.
[37] M. C. Stuparu, A. Khan, *J. Polym. Sci., Part A: Polym. Chem.* **2016**, *54*, 3057.
[38] Y. Liu, W. Hou, H. Sun, C. Cui, L. Zhang, Y. Jiang, Y. Wu, Y. Wang, J. Li, B. S. Sumerlin, Q. Liu, W. Tan, *Chem. Sci.* **2017**, *8*, 6182.
[39] L. Martínez-Jothar, S. Doulkeridou, R. M. Schiffelers, J. Sastre Torano, S. Oliveira, C. F. van Nostrum, W. E. Hennink, *J. Controlled Release* **2018**, *282*, 101.
[40] M. F. Debets, W. P. J. Leenders, K. Verrijp, M. Zonjee, S. A. Meeuwissen, I. Otte-Höller, J. C. M. van Hest, *Macromol. Biosci.* **2013**, *13*, 938.
[41] P. Gobbo, Z. Mossman, A. Nazemi, A. Niaux, M. C. Biesinger, E. R. Gillies, M. S. Workentin, *J. Mater. Chem.* **2014**, *2*, 1764.
[42] J. Gaitzsch, D. Appelhans, L. Wang, G. Battaglia, B. Voit, *Angew. Chem., Int. Ed.* **2012**, *51*, 4448.
[43] D. Grafe, J. Gaitzsch, D. Appelhans, B. Voit, *Nanoscale* **2014**, *6*, 10752.
[44] X. Liu, P. Formanek, B. Voit, D. Appelhans, *Angew. Chem.* **2017**, *129*, 16451.
[45] X. Liu, D. Appelhans, B. Voit, *J. Am. Chem. Soc.* **2018**, *140*, 16106.
[46] S. Moreno, P. Sharan, J. Engelke, H. Gumz, S. Boye, U. Oertel, P. Wang, S. Banerjee, R. Klajn, B. Voit, A. Lederer, D. Appelhans, *Small* **2020**, *16*, 2002135.
[47] S. Varlas, J. C. Foster, P. G. Georgiou, R. Keogh, J. T. Husband, D. S. Williams, R. K. O'Reilly, *Nanoscale* **2019**, *11*, 12643.
[48] C. G. Palivan, R. Goers, A. Najer, X. Zhang, A. Car, W. Meier, *Chem. Soc. Rev.* **2016**, *45*, 377.
[49] P. Wen, X. Wang, S. Moreno, S. Boye, D. Voigt, B. Voit, X. Huang, D. Appelhans, *Small* **2021**, *17*, 2005749.

[50] E. Geervliet, S. Moreno, L. Baiamonte, R. Booijink, S. Boye, P. Wang, B. Voit, A. Lederer, D. Appelhans, R. Bansal, *J. Controlled Release* **2021**, *332*, 594.
[51] B. Iyisan, J. r. Kluge, P. Formanek, B. Voit, D. Appelhans, *Chem. Mater.* **2016**, *28*, 1513.
[52] B. Iyisan, A. C. Siedel, H. Gumz, M. Yassin, J. Kluge, J. Gaitzsch, P. Formanek, S. Moreno, B. Voit, D. Appelhans, *Macromol. Rapid Commun.* **2017**, *38*, 1700486.
[53] C. K. Wong, A. J. Laos, A. H. Soeriyadi, J. Wiedenmann, P. M. Curmi, J. J. Gooding, C. P. Marquis, M. H. Stenzel, P. Thordarson, *Angew. Chem.* **2015**, *127*, 5407.
[54] J. Zhu, X. Xu, M. Hu, L. Qiu, *J. Biomed. Nanotechnol.* **2015**, *11*, 997.
[55] H. Chun, M. Yeom, H.-O. Kim, J.-W. Lim, W. Na, G. Park, C. Park, A. Kang, D. Yun, J. Kim, D. Song, S. Haam, *Polym. Chem.* **2018**, *9*, 2116.
[56] S. Chen, J. Qin, J. Du, *Macromolecules* **2020**, *53*, 3978.
[57] J. d. A. Pachioni-Vasconcelos, A. M. Lopes, A. C. Apolinário, J. K. Valenzuela-Oses, J. S. R. Costa, L. d. O. Nascimento, A. Pessoa, L. R. S. Barbosa, C. D. O. Rangel-Yagui, *Biomater. Sci.* **2016**, *4*, 205.
[58] A. Najer, D. Wu, D. Vasquez, C. G. Palivan, W. Meier, *Nanomedicine* **2013**, *8*, 425.
[59] J. F. Mukerabigwi, Z. Ge, K. Kataoka, *Chem. - Eur. J.* **2018**, *24*, 15706.
[60] K. B. Joshi, S. Verma, *Biophys. Chem.* **2009**, *140*, 129.
[61] P. Kuhn, K. Eyer, T. Robinson, F. I. Schmidt, J. Mercer, P. S. Dittrich, *Integr. Biol.* **2012**, *4*, 1550.
[62] D. Wu, S. Rigo, S. Di Leone, A. Belluati, E. C. Constable, C. E. Housecroft, C. G. Palivan, *Nanoscale* **2020**, *12*, 1551.
[63] P. Ascenzi, A. di Masi, G. Fanali, M. Fasano, *Cell Death Discovery.* **2015**, *1*, 15025.
[64] U. L. Muza, S. Boye, A. Lederer, *Anal. Sci. Adv.* **2021**, *2*, 95.
[65] H. Gumz, S. Boye, B. Iyisan, V. Krönert, P. Formanek, B. Voit, A. Lederer, D. Appelhans, *Adv. Sci.* **2019**, *6*, 1801299.
[66] S. Moreno, S. Boye, A. Lederer, A. Falanga, S. Galdiero, S. Lecommandoux, B. Voit, D. Appelhans, *Biomacromolecules* **2020**, *21*, 5162.
[67] R. Ccorahua, S. Moreno, H. Gumz, K. Sahre, B. Voit, D. Appelhans, *RSC Adv.* **2018**, *8*, 25436.
[68] A. Jain, K. Cheng, *J. Controlled Release* **2017**, *245*, 27.
[69] T. Komatsu, *Nanoscale* **2012**, *4*, 1910.
[70] A. Jain, A. Barve, Z. Zhao, W. Jin, K. Cheng, *Mol. Pharmaceutics* **2017**, *14*, 1517.